Influences of inert gas electric arc spraying parameters on the porosity of Cp Ti coating on Titanium alloy (Ti-6Al-4V) using response surface methodology

Ashwinkumar V Patel
Associate Professor
Mechanical Engineering Department,
Government Engineering College, Valsad, India

Abstract: The number of total hip arthroplasties (THA) operations is increasing, reaching more than one million procedures worldwide per year. The advent of porous coatings for joint replacement prostheses has proven to be a remarkable innovation in the field of orthopedics. These coatings allow for biologic fixation of implants to host bone via ingrowth into the integrated porous structure. The ability of bone to remodel around cementless prostheses may attribute to enhance long-term success with these components. The impetus to develop porous materials initially arose from concerns regarding late aseptic loosening found with cemented hip replacements. Porous metallic coatings on cementless femoral stem for improved osseointegration have gained momentum since last two decades. In this research twin wire arc spraying technique is used with argon as inert gas to obtain porosity in the range of 30 % - 40 % which is suitable for faster osseointegration. The optimum process parameters i.e. power, stand-off distance and wire feed rate are obtained using response surface methodology technique.

Index Terms- Twin-wire electric arc spraying, porosity, power, stand-off distance, wire feed rate, response surface methodology

I. INTRODUCTION

Twin-wire arc spraying is chosen as the method to deposit the coating on the components for various reasons. This method is used to deposit coating for corrosion resistance, wear, and friction resistance. Generally, plasma spray coating is used for porous coating on the biomedical implant. The drawbacks of this coating like thermal distortion of the substrate, residual stress at high temperature in the coating, high-temperature oxidation lead to new methods like twin wire electric arc spray coating as a low-cost alternative [1]. This method is generally used with compressed air, nitrogen or argon. In this research argon which is inert in nature, is used as a carrier gas for this process.

Porous coating of the orthopedic implant with porosity in the range of 30 % - 40 % is the necessary requirement for the load-bearing orthopedic implant for faster osseointegration. Coating characteristics like porosity, pore size, microhardness, etc. depends upon the process parameters of any thermal spray process [2]. In this paper, the influence of processing parameters on the porosity of inert gas-electric arc spraying has been studied and the required porosity is obtained by combining suitable input process parameters.

II. MATERIAL & METHODS

a) IDENTIFICATION OF IMPORTANT PROCESSING PARAMETERS

From the literature survey and the investigation done in our laboratory, the important factors (process parameters of electric arc spray) which have a greater effect on the properties of the coating were identified. These process parameters are (i) P (power in kW), (ii) S (stand-off distance in mm) and (iii) F (wire feed rate in m/min.

b) WORKING RANGE OF THE PROCESS PARAMETERS

50 pieces of 12 mm (dia.) × 10 mm (height) was cut from the Ti alloy (Ti-6Al-4V) rod. Grit blasting was done on the cut section surface of specimens using cabinet type grit blasting machine. Grit blasting was done using abrasive alumina (Al2O3) grits of size 250 ± 30 μm. The specimens then cleaned in an ultrasonic bath using acetone and dried. Some trial spray runs were conducted on samples to decide the practical working range of electric arc spraying parameters. The thickness of the coating for all the samples

was maintained at 350 ± 15 µm. The P (power), S (stand-off distance) and F (wire feed rate) were examined to decide the working limits of these input spray parameters for the electric arc spray process. This leads to the following judgments:

I. If the arc spray was done below 3.4 kW power, then partial melting of wires and poor adhesion occurred. If the arc spray was done above 12.6 kW power, then spattering and poor efficiency of deposition were observed.

II. If the arc spray was done at < 100 mm stand-off distance, then the short arc length produced and the feeding of wire became inconvenient. If the arc spray was done at > 300 mm, arc wandering and instability of arc were noticed because of increased length of the arc.

III. The lowest possible feed rate of wire was 0.94 m/min (limitation of the system for wire feeding). If the feed rate of wire > 3.0 m/min, the deposition of the coating was very rough because of the partial melting of the wires. Argon is used as the carrier gas. For all the coatings produced here, the argon gas flow rate was maintained constant.

c) DEVELOPING THE DESIGN MATRIX

Considering all of the above-mentioned conditions, the practical limits of the processing parameters were selected in this manner that the Ti alloy (Ti-6Al-4V) samples can be coated easily. Three factors, five levels CCD (central composite design) matrix was selected to optimize the variations in the experimental results. To achieve the aforesaid aim, a factorial technique was used to design the experiments statistically to decrease the cost and time. The main and interaction effects of input parameters (P, S, and F) on the response (output) parameters could be easily obtained. In RSM (Response surface methodology), CCD (second-order) was observed to be the most efficient statistical tool. It was used to establish the mathematical relation of the response surface. It used the lowest possible number of experiments without losing its accuracy [3]. Table 1 shows the range of input factors considered and Table 2 highlights the parameters of the electric arc spray process used for Cp Ti coatings on Ti alloy (Ti-6Al-4V). The design matrix is shown in Table 3. Twenty sets of coded conditions included in this design matrix. It consists of 8 points with a three-factor fully replicated factorial design, 6 corner points, and 6 center points. All three process variables at the middle (0) level creates the center points while the combinations of each input process parameters at either the highest (+1.682) or the lowest (-1.682) value or with the other variables at the intermediate levels make the star points. Therefore, the twenty experimental runs permitted to estimate the linear, quadratic, and two-way interactive effects of the variables on the Cp Ti coating. The literature [4, 5] are dealt with the way of designing such a matrix. For the ease of recording and processing data of experimentation, the lower and upper levels of the input factors have been coded as -1.682 and +1.682, respectively. The coded values of the intermediate points can be obtained by using the following equation:

$$Xi = 1.682 \times \frac{[2X - (Xmax + Xmin)]}{(Xmax - Xmin)} \quad (1)$$

Where Xi is the coded value of a variable X which is required and X is the value of the variable anywhere from Xmin to Xmax; Xmin = lower value of the variable, ‘X’; and Xmax = upper value of the variable, ‘X’.

d) EXPERIMENTAL INVESTIGATIONS

In this investigation, 20 coated samples were made with different combinations of electric arc spraying parameters, as given by the experimental design matrix (Table 3). The experiments were performed in an arbitrary order to avoid systematic errors infiltrating from the system. As per the ASTM F1854 standard [6], the porosity value of the coating was calculated using the polished cross-section. An optical microscope equipped with an image analyzing system was used for this purpose.

Table 1 Important electric arc spray process parameters and their levels

Factors	Notations	Units	Levels				
			-1.682	-1	0	1	+1.682
Power	P	kW	3.4	5.4	7.6	10	12.6
Stand-off distance	S	cm	100	150	200	250	300
Wire feed rate	F	m/min	0.94	1.30	1.86	2.51	3.01

Table 2 Constant parameters during electric arc spraying

Parameters	Unit	Values
Supply voltage (3 Phase)	V	415
Wire diameter (Cp Ti)	mm	2
Air Pressure	bar	5.5
Primary gas flow rate	m3/min	2 (free air delivery)

Table 3 Design matrix and experimental results

Spray condition	Coded values			Original value			Measured Porosity values of coatings (vol %)
	P	S	F	P (kW)	S (mm)	F (m/min)	
1	-1	-1	-1	5.4	150	1.3	36.6
2	1	-1	-1	10	150	1.3	32
3	-1	1	-1	5.4	250	1.3	37
4	1	1	-1	10	250	1.3	32.42
5	-1	-1	1	5.4	150	2.51	35.4
6	1	-1	1	10	250	2.51	33.02
7	-1	1	1	5.4	250	2.51	39
8	1	1	1	10	250	2.51	36.75
9	-1.682	0	0	3.4	200	1.86	37.1
10	1.682	0	0	12.6	200	1.86	33
11	0	-1.682	0	7.6	100	1.86	33.42
12	0	1.682	0	7.6	300	1.86	37
13	0	0	-1.682	7.6	200	0.94	34.21
14	0	0	1.682	7.6	200	3.01	36.5
15	0	0	0	7.6	200	1.86	31.15

16	0	0	0	7.6	200	1.86	30.42
17	0	0	0	7.6	200	1.86	31.15
18	0	0	0	7.6	200	1.86	31
19	0	0	0	7.6	200	1.86	31.15
20	0	0	0	7.6	200	1.86	31.3

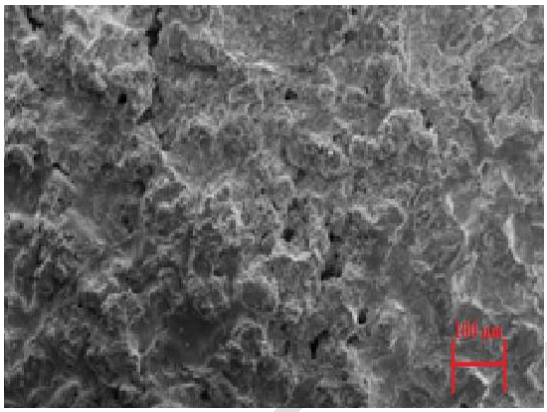

Figure 1 SEM image of the top surface of Cp Ti coating

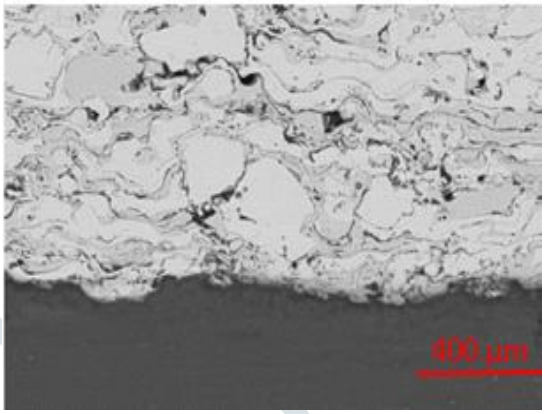

Figure 2 Backscattered cross-sectional SEM image of Cp Ti coating

e) COATING MORPHOLOGIES

The top surface of the Cp Ti coating is shown in the SEM image (Figure 1). It revealed a very uneven surface. The pores are interconnected and distributed inside the layer. The backscattered SEM image shows good attachment at the coating/ substrate interface (Figure 2). The phase composition of the coating was measured by Rigaku Ultima IV, X-ray diffractometer using CuKa radiation which was set at 40 kV and 20 mA for the XRD analysis. The data were recorded in the 2θ range 200 to 800 in steps of 20/min. The XRD pattern of the Cp Ti wire exhibit α-Ti phase only as seen in Figure 3, whereas the XRD pattern of the sprayed coating shows both α-Ti and β-Ti phases as shown in Figure 4.

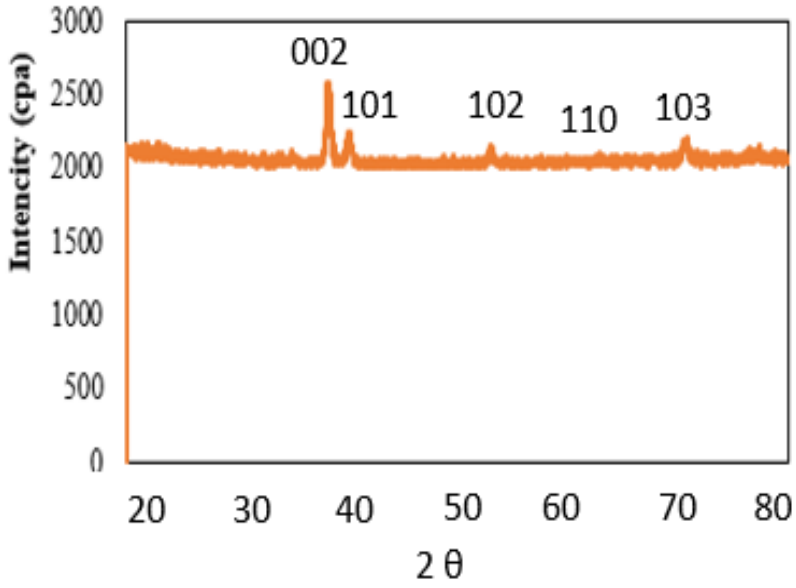

Figure 3 XRD pattern of the Cp Ti Wire

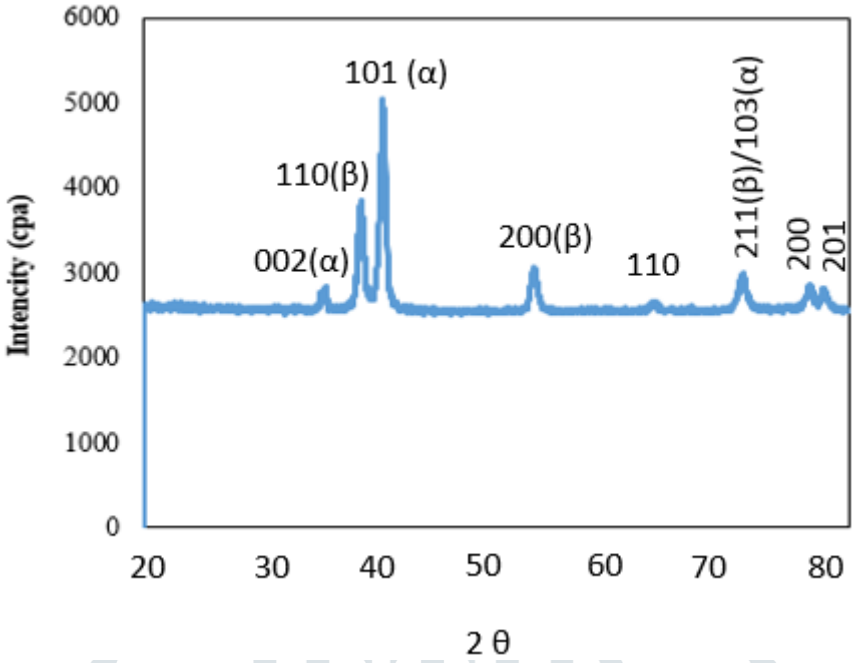

Figure 4 XRD pattern of the Titanium alloy substrate

f) DEVELOPING AN EMPIRICAL RELATIONSHIP

As the porosity is a function of power (P), stand-off distance(S), wire feed rate (F) and hence it can be measurably expressed as;

Porosity (PL) = f (P, S, F) (2)

The second-order polynomial (regression) equation to represent the response surface Y (Porosity) can be given by;

$$Y = b0 + \Sigma\, bi\, Xi + \Sigma\, bii\, Xi2 + \Sigma\, bij\, Xi\, Xj \quad (3)$$

and for three factors, the selected polynomial could be expressed as

Porosity (PL) = bo + b1 × (P) + b2 × (S) + b3 × (F) + b11 × (P2) + b22 × (S2) + b33 × (F2) + b12 × (PS) + b13 × (PF) + b23 × (SF) (4)

Where b0 is the average of the responses and b1, b2, b3, b11, b12, b13 …b22, b23, b33, are regression coefficients that depend on respective linear, interaction, and squared terms of factors. The value of these coefficients was calculated using Minitab 17.0 software. The significance of each coefficient was determined by Student's't' test and 'p-values', which are listed in Table 4. Values of ''Prob > fisher ratio (F)'' less than 0.0500 indicate that model terms are significant. In this case, P, S, F, PS, PF, SF, P2, S2, and F2 are significant model terms. Values greater than 0.1000 indicate that the related terms are not significant. The results of multiple linear regression coefficients for the second-order response surface model are given in Table 5

Table 4 ANOVA test results

Source	Sum of squares	df	Mean square	F value	p-Value Prob >F	
Model	135.961	9	15.1076	101.74	< 0.0001	Significant
P	31.392	1	31.3917	211.42	< 0.0001	Significant
S	14.704	1	14.7041	99.03	< 0.0001	Significant
F	7.324	1	7.3242	49.33	< 0.0001	Significant
PS	0.003	1	0.0028	0.02	0.893	Not significant

PF	2.588	1	2.5878	17.43	0.002	Not significant
SF	5.298	1	5.2975	35.68	< 0.0001	Significant
P2	27.561	1	27.5610	185.62	< 0.0001	Significant
S2	29.862	1	29.8619	201.12	< 0.0001	Significant
F2	32.027	1	32.0268	215.70	< 0.0001	Significant
Residual	1.485	10	0.1485			
Lack of fit	0.996	5	0.1991	2.04	0.227	Not significant
Pure error	0.489	5	0.0978			
Cor. total	137.445	19				
Std. dev.	0.385329					
Mean	34.00					
C.V %	2.50					
Press	9.185101					
Adeq precision	37.25676					

df: degrees of freedom; F: Fisher ratio; p: probability

R-squared =0.9892, Adj R-squared = 0.9795, Pred R-squared = 95.89

Table 5 Estimated regression coefficients

Factor	Estimated coefficient
Intercept	31.034
P–P	-1.516
S–S	1.038
F–F	0.732
PS	0.019
PF	0.569
SF	0.814
P2	1.383
S2	1.439
F2	1.491

The final empirical relationship was constructed using only these coefficients, and the developed final empirical relationship in coded condition is given below.

$$\text{Porosity (PL)} = \{31.034 - 1.516 \times (P) + 1.038 \times (S) - 0.732 \times (F) + 0.019\,(P\times S) + 0.569 \times (P\times F) + 0.814 \times (S\times F) + 1.383 \times P2 + 1.439 \times (S2) + 1.491 \times (F2)\}\ (\text{vol \%}) \quad (5)$$

ANOVA technique was used to check the adequacy of the developed empirical relationship [9]. In this investigation, the desired level of confidence was considered to be 95%. The relationship may be considered to be adequate provided that (a) the calculated value of the F ratio of the model developed should not exceed the standard tabulated value of 'F' ratio and (b) the calculated value of the 'R' ratio of the developed relationship should exceed the standard tabulated value of 'R' ratio for a desired level of confidence. It is found that the model is adequate. The model F value of 101.74 implies that the model is significant. There is only a 0.01% chance that a model F value this large could occur due to noise. The lack of fit F value of 0.6995 implies that the lack of fit is insignificant. There is only a 0.05% chance that a lack of fit F value this large could occur due to noise. The normal probability plot of the residuals for porosity shown in Figure 5 revealed that the residuals are falling on the straight line, which means the errors are distributed normally. All the above consideration indicates the adequacy of the developed relationship. Each predicted value matches its experimental value as shown in Figure 6. The Fisher's F test with a very low probability value (Pmodel > F= 0.0001) demonstrates a very high significance for the regression model. The goodness of fit of the model was checked by the determination coefficient (R2). The coefficient of determination (R2) was calculated to be 0.9892 for response. This implies that 98.92% of experimental data confirms the compatibility with the data predicted by the model, and the model does not explain only 0.925% of the total variations. The R2 value is always between 0 and 1, and its value indicates aptness of the model. For a good statistical model, R2 value should be close to 1.0.The adjusted R2 value reconstructs the expression with the significant terms. The value of the adjusted determination coefficient (Adj. R2 = 0.9795) is also high to advocate for a high significance of the model. The Pred. R2 is 0.9589 that implies that the model could explain 96% of the variability in predicting new observations. The value of coefficient of variation is also low as 5.174 indicates that the deviations between experimental and predicted values are low. Adeq. precision measures the signal to noise ratio. A ratio greater than 4 is desirable. In this investigation, the ratio is 37.25, which indicates an adequate signal. This model can therefore be used to navigate a design space with certainty.

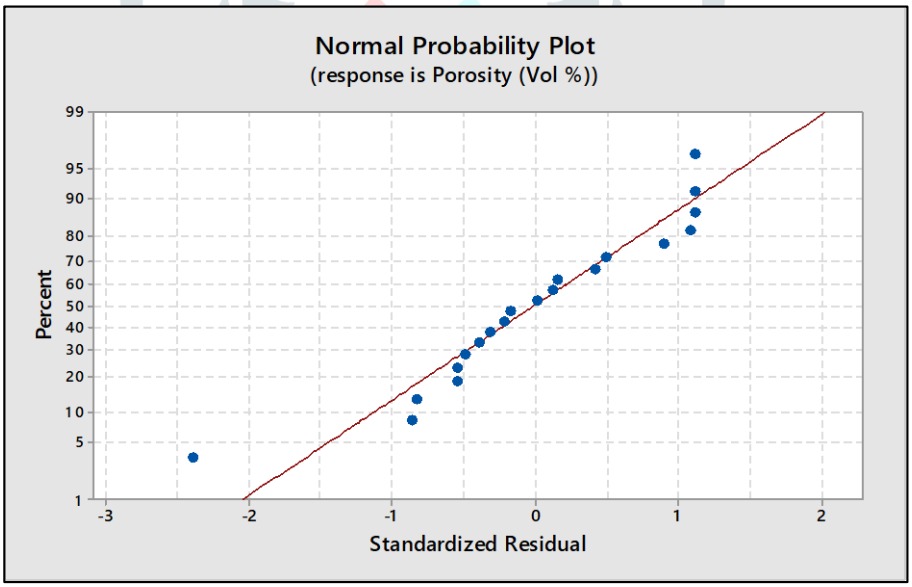

Figure 5 Normal probability plot for porosity

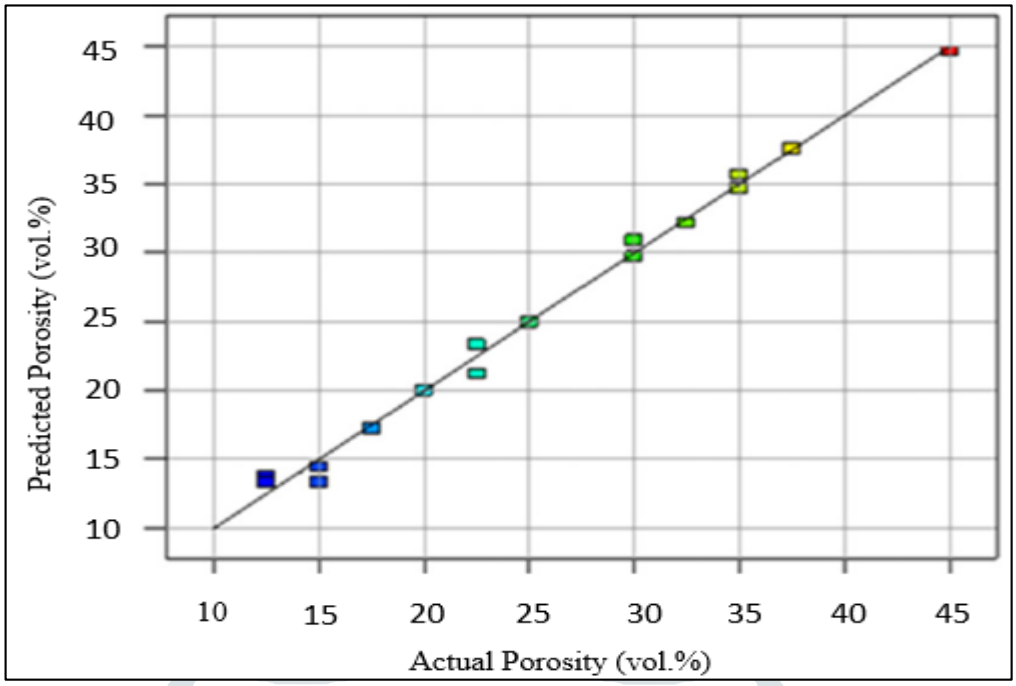

Figure 6 Correlation graph for porosity

III. OPTIMIZING THE ELECTRIC ARC SPRAYING PARAMETERS

The response surface methodology (RSM) was used to optimize the parameters in this study. RSM is a collection of mathematical and statistical techniques that are useful for designing a set of experiments, developing a mathematical model, analyzing for the optimum combination of input parameters, and expressing the values graphically [7]. To obtain the influencing nature and optimized condition of the process on porosity, the surface plots and contour plots which are any indications of possible independence of factors have been developed for the proposed empirical relation by considering two parameters in the middle level and two parameters in the x and y axes as shown in Figure 7. These response contours can help in the prediction of the response (P) for any zone of the experimental domain [8]. The valley (trough) of the response plot shows the minimum achievable porosity. A contour plot is produced to display the region of the optimal factor settings visually. For second-order responses, such a plot can be more complex compared to the simple series of parallel lines that can occur with first-order models. Once the stationary point is found, it is usually necessary to characterize the response surface in the immediate vicinity of the point. Characterization involves identifying whether the stationary point is a minimum response or maximum response or a saddle point. To classify this, it is most straightforward to examine it through the contour plot. Contour plots, therefore, play a very important role in the study of a response surface. It is clear from Figure 7 that the porosity decreases, and increases with the increase in the levels of considered process parameters. By analyzing the response surfaces and contour plots (Figure 7), the maximum achievable porosity value is found to be 36.75 vol%. The corresponding parameters that yielded the value are input power of 7.6 kW, stand-off distance of 250 mm and wire feed rate of 1.86 m/min. To validate the model, three additional confirmation experiments were conducted to compare the experimental results with the prediction under the optimal conditions. The mean experimental porosity level obtained as 34.23 vol%. The error percentage of 3.7 % showed an excellent prediction of the model. The coating produced under optimized spray parameters is shown in Figure 8. From the figure, it could be inferred that the coatings fine structured and homogenous morphology with high porosities. Contributions made by the process parameters on porosity can be ranked [9, 10] from their respective F ratio value which is seen in Table 4 which provided the degrees of freedom for all the input parameters. The higher F ratio value implies that the respective term is more significant and vice versa. From the F ratio values, it can be concluded that input power is contributing more on porosity of the Cp Ti coating, and it is followed by stand-off distance, and wire feed rate for the range considered in this investigation.

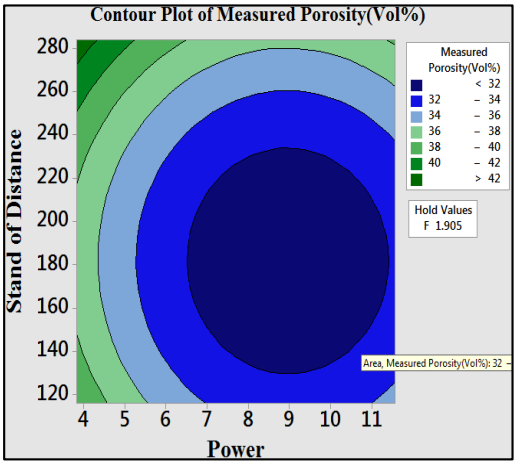

(a) Contour plot of power and stand-off distance

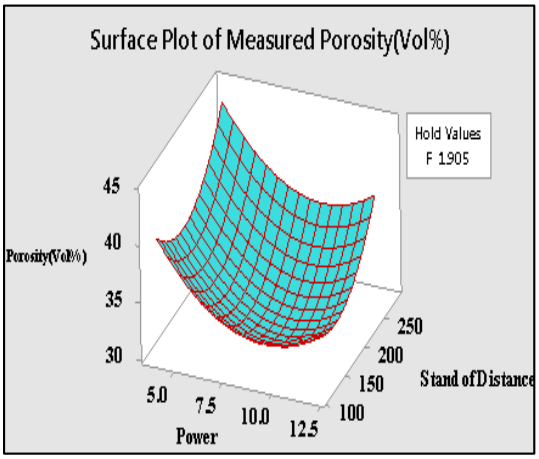

(b) Surface plot of power and stand off distance

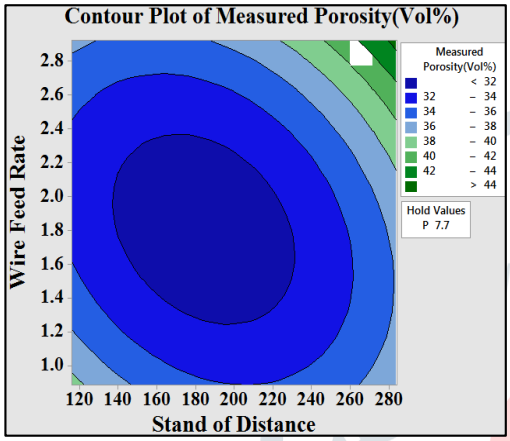

(c) Contour plot of stand-off distance and wire feed rate

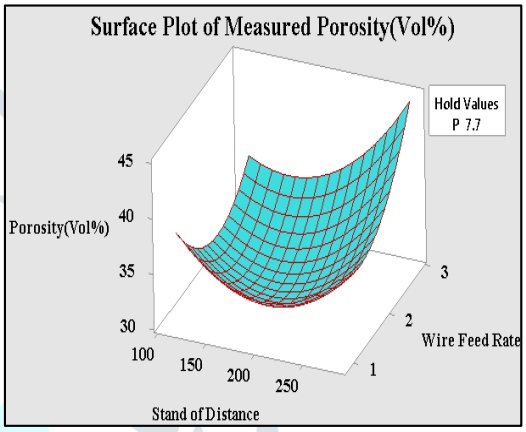

(d) Surface plot of stand-off distance and wire feed rate

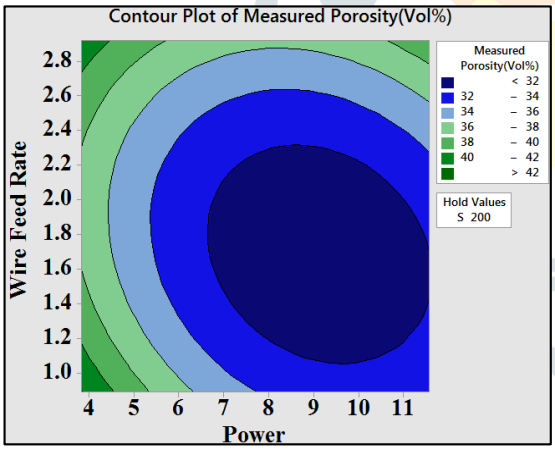

(e) Contour plot of power and wire feed rate

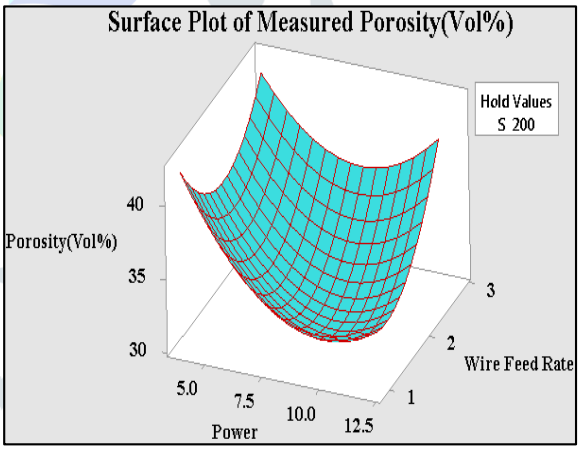

(f) Surface plot of power and wire feed rate

Figure 7 Response graphs and contour plots

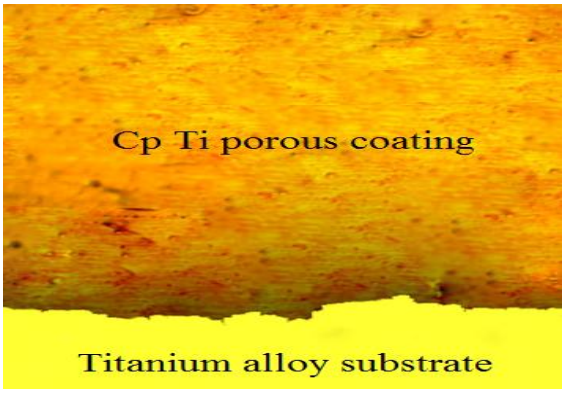

Figure 8 Optical micrograph of a cross section of the coating deposited under optimized spray parameters.

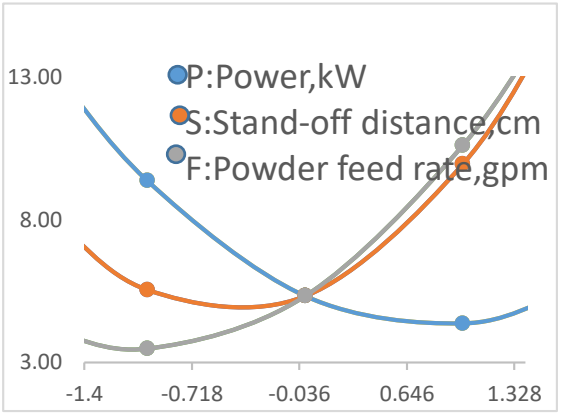

Figure 9 Perturbation plot for porosity.

IV. RESULTS AND DISCUSSION

'Perturbation plot shown in Figure 9 illustrates the effect of the electric arc spraying parameters on the responses for an optimization design. This graph shows how the response changes as each factor moves from a chosen reference point, with all other factors held constant at the reference value. A steep slope or curvature in a factor indicates that the response is sensitive to that factor. A relatively flat line shows insensitivity to change in that particular factor.

a) EFFECT OF INPUT POWER ON POROSITY

The influence of input power (curve P) on the porosity of the coatings are displayed in Figure 7 to Figure 9). From the figure, it can be inferred that the input power has an inversely proportional relationship with the porosity. The spraying power is an important parameter that affects the quality of the coating, since it can influence the temperature and velocity of the wire particles at the moment of striking the substrate. More complete particle melting usually results in lower porosity content. At low spraying powers, the wire particles are poorly melted. When they impact on the substrate or the already formed coating, they are not able to spread out completely to form splats and therefore, could not conform to the surface. In such a case, the interlamellar pores and cracks will be formed due to the solidification of the splats [11]. Moreover, when the spraying power is relatively low, numerous unmelted and partially melted particles exist in the coating. During the cooling process after spraying, the micro- cracks and pores are formed near the boundary of the unmelted particle, since the material mismatch between the unmelted particles and around the splats occurs, as shown in Figure 10 (a). At the boundary of the unmelted particles, the micro-cracks do often exist. Unmelted particles are produced when the injected wire particles do not melt completely in the electric arc or do melt but subsequently resolidify before impact. For a given size distribution of the wire, if the thermal energy transferred to the particles in the electric arc is not sufficient to produce a fully molten droplet, the resulting droplets will not completely flatten out and bond well with the underlying surface. Unmelted particles are serious defects in such thermal spray coatings. The above results indicate that, the low spraying power cannot provide enough energy to melt the particles. When the power is high, the fully melted Cp Ti is considered to be well distributed and infiltrated in the splat boundary [12]. When the power is sufficiently high, most of the wire particles have been melted and the flow ability of splats is good as shown in Figure 10 (b).

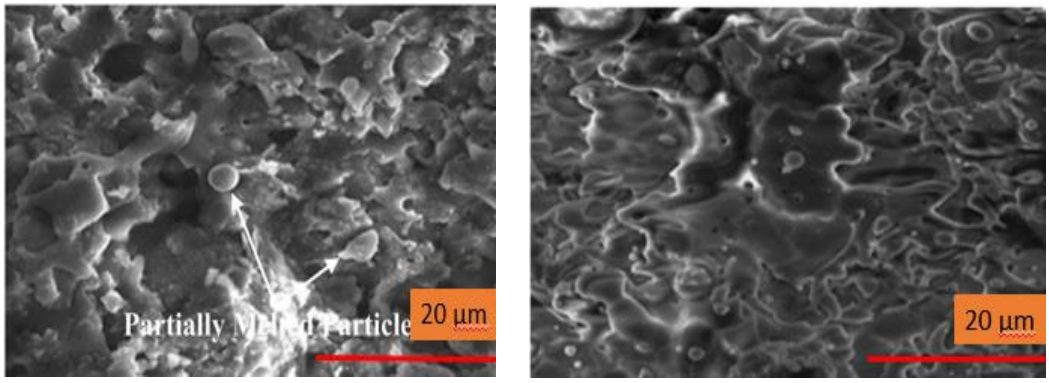

(a) 3.4 kW (lowest) (b) 12.6 kW (highest)

Figure 10 Effect of input power on porosity

b) EFFECT OF STAND-OFF DISTANCE ON POROSITY

The effect of stand-off distance (curve S) on porosity of the coatings is exhibited in Figure 9. It can be inferred that the stand-off distance has a directly proportional relationship with the porosity. The crystallinity of the Cp Ti coatings increases as the spraying distance decreases mainly due to the increase in the droplet temperature at the moment of impingement. At short spraying distance, the droplets strike the substrate are semi or fully melted and as a result the Cp Ti phase become more crystalline because the solidification rate gradually decreases as the coating thickness increases (Figure 11 (a)).The stand-off distance mainly controls the cohesion between splats because the temperature and velocity of particles in the electric arc flame significantly changes with stand-off distance. Therefore, better spreading and cohesion would be achieved with shorter spraying distances. With a longer spray distance, the sprayed molten particles have more time to react with the air/gas entrained in the flame, which would result in an increase in oxide content with spray distance. The coatings deposited at a spraying distance of 300 mm were found to contain fewer unmelted particles and lower porosity than the trends would have suggested. Porosity in the coatings increased with the increase in spray distance. It has been reported that the longer spray distance increases the dwell time in the plume and allows more thorough heating/melting of the particles and the enthalpy of the molten particles is largely lost, and the particles slow down in a relatively longer flight path. Under such conditions, the particles arriving on the substrate will not be sufficiently flattened to overlap the layers, resulting in porosity as shown in Figure 11 (b). At shorter and longer spray distance, the particles remain unmelted or partially melted and surface roughness and porosity increases. Therefore there is a need to optimize the stand-off distance for consistency and reliability of coatings.

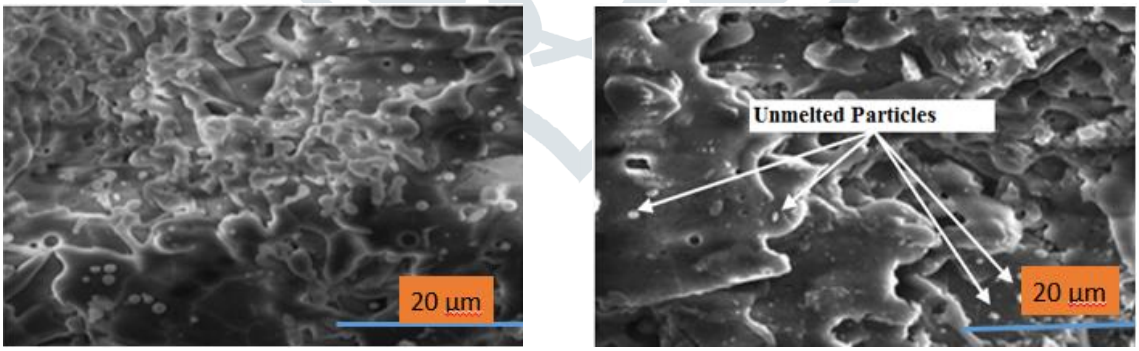

(a) 100 mm (lowest) (b) 300 mm (highest)

Figure 11 Effect of stand-off distance on porosity

c) EFFECT OF WIRE FEED RATE ON POROSITY

The effect of wire feed rate (curve F) on the response of the coatings is revealed in Figure 9. During electric arc spraying, the interaction between the gas flow and particles, the particle's velocity and temperature are influenced by the wire feed rate. From Figure 12 (a) it could be inferred that, when the wire feed rate value is low, the splats poorly flattens and spread out. There are numerous pores existing at the boundaries of overlapping splats. Moreover, the cohesive strength between the adjacent splats is low since the micro-cracks are visible at the interface [13]. When the wire feed rate is extremely low (e.g., 0.94 m/min), most of particles

are fully melted. In such a case, the coating with dense microstructure and low porosity get fabricated. When the wire feed rate is in a range between 0.94 m/min and 1.30 m/min, the amount of the pores and micro-cracks increases with increasing the wire feed rate. The existence of these pores and micro-cracks with different dimensions lead to increases the porosity of the coating. However, when the wire feed rate is very high, the amount of the unmelted and partially melted particles in the coating increases with increasing wire feed rate. At high wire feed rate, the heat content in the electric arc gas becomes inadequate for the melting of the wire particles [14]. At the boundary of the unmelted particle, the micro-cracks and pores are found. These micro-cracks and pores may be created due to the residual stress arising from the material mismatch of unmelted particles and the splats in a molten state. The poorly melted (unmelted and partially melted) particles will remain in the coating, resulting in a less-dense coating with high porosity (Figure 12 (b)). This result indicates that, when the wire feed rate is high, the particles which obtain low thermal energy and kinetic energy cannot be fully melted and hence again it is desirable to optimize this parameter for consistency and reliability of the coatings.

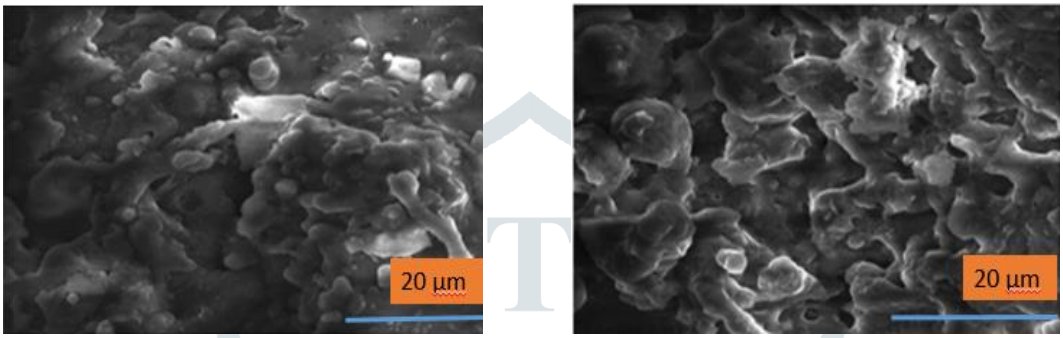

(a) 0.94 m/min (lowest) (b) 3.01 m/min (highest)

Figure 12 Effect of wire feed rate on porosity

d) SENSITIVITY ANALYSIS

Sensitivity analysis is a method to identify critical parameters and rank them by their order of importance. This is paramount in model validation where attempts are made to compare the calculated output to the measured data. This type of analysis can be useful to find out, which input parameter must be most accurately measured, thus determining the input parameters exerting an influence upon the model outputs [15]. Mathematically, sensitivity of a design objective function with respect to a design variable is the partial derivative of that function with respect to its variables. To obtain the sensitivity equation for input power, Eq. (5) with non-significant terms is differentiated with respect to input power. The sensitivity Eqs. (6)– (8) represent the sensitivity of porosity for input power, stand-off distance and wire feed rate, respectively.

$$\frac{\partial PL}{\partial P} = -1.516 - 0.019 \times S + 0.569 \times F + 2.766 \times P \quad (6)$$

$$\frac{\partial PL}{\partial S} = 1.038 + 0.019 \times P + 0.814 \times F + 2.878 \times S \quad (7)$$

$$\frac{\partial PL}{\partial F} = 0.732 + 0.569 \times P + 0.814 \times S + 2.982 \times F \quad (8)$$

In this analysis, the aim is to predict the tendency of porosity due to a small change in process parameters of electric arc spraying process. Sensitivity information should be interpreted using mathematical definition of derivatives. Namely, positive sensitivity values imply an increment in the objective function by a small change in design parameter, whereas, negative values state the opposite. In Figure 13, Figure 14 &

Figure 15) the input power, stand-off distance and wire feed rate sensitivity maps on porosity are displayed respectively. The small variation of input power causes large changes in porosity. The results reveal that the porosity is more sensitive to input power than stand-off distance and wire feed rate.

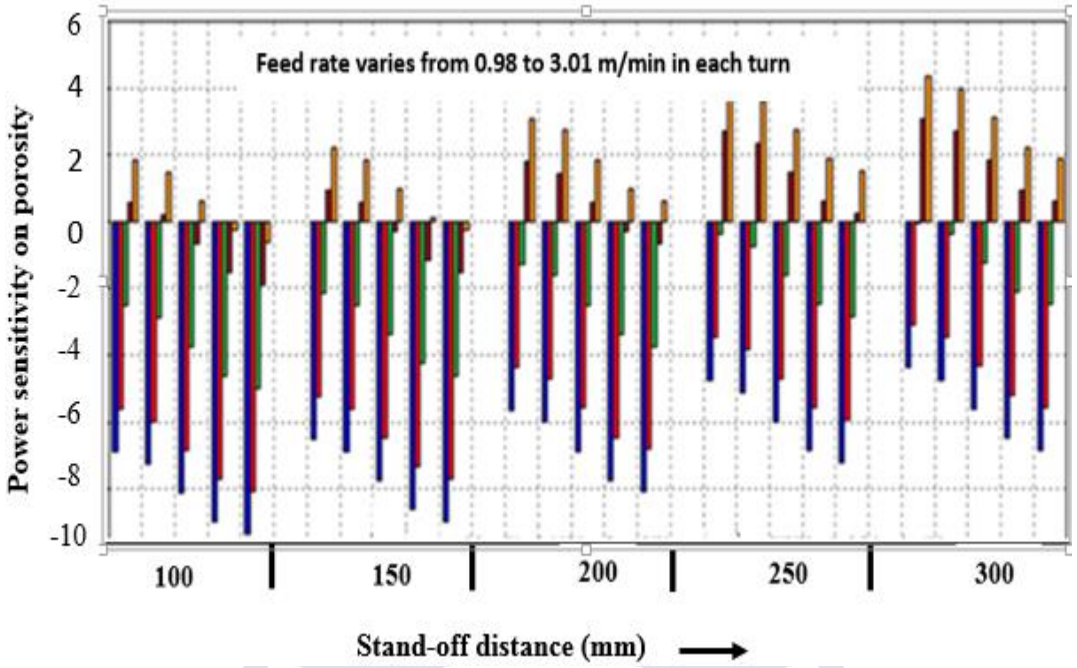

Figure 13 Input power sensitivity of porosity

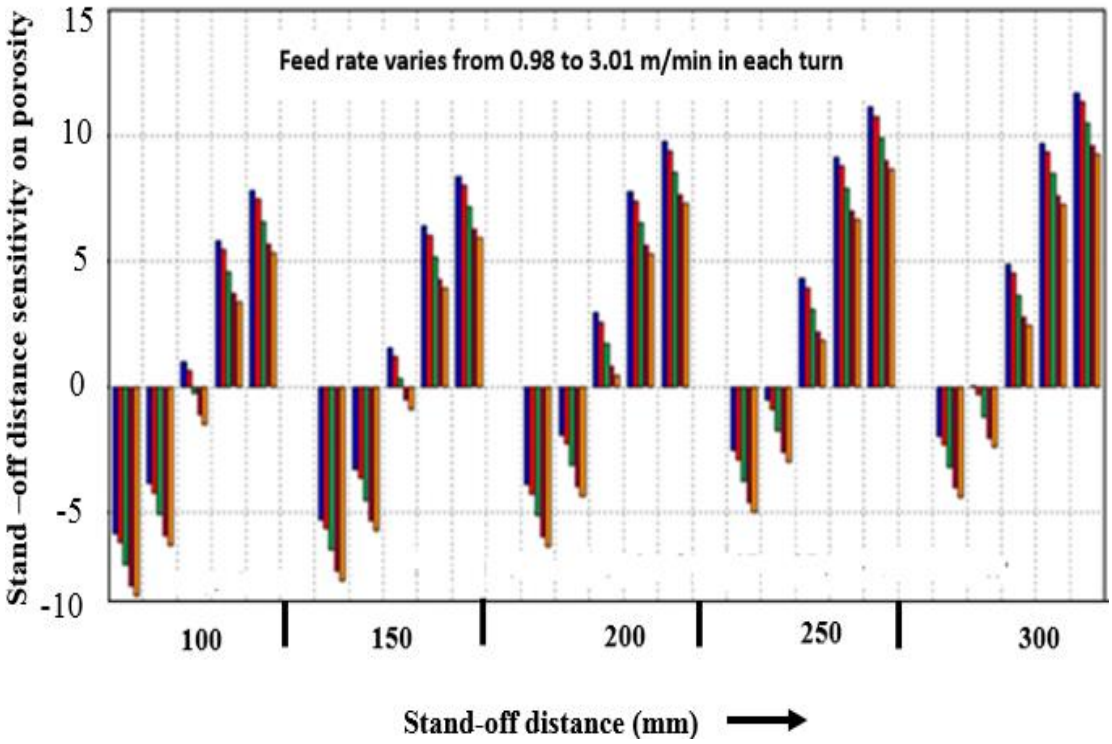

Figure 14 Stand-off distance sensitivity of porosity

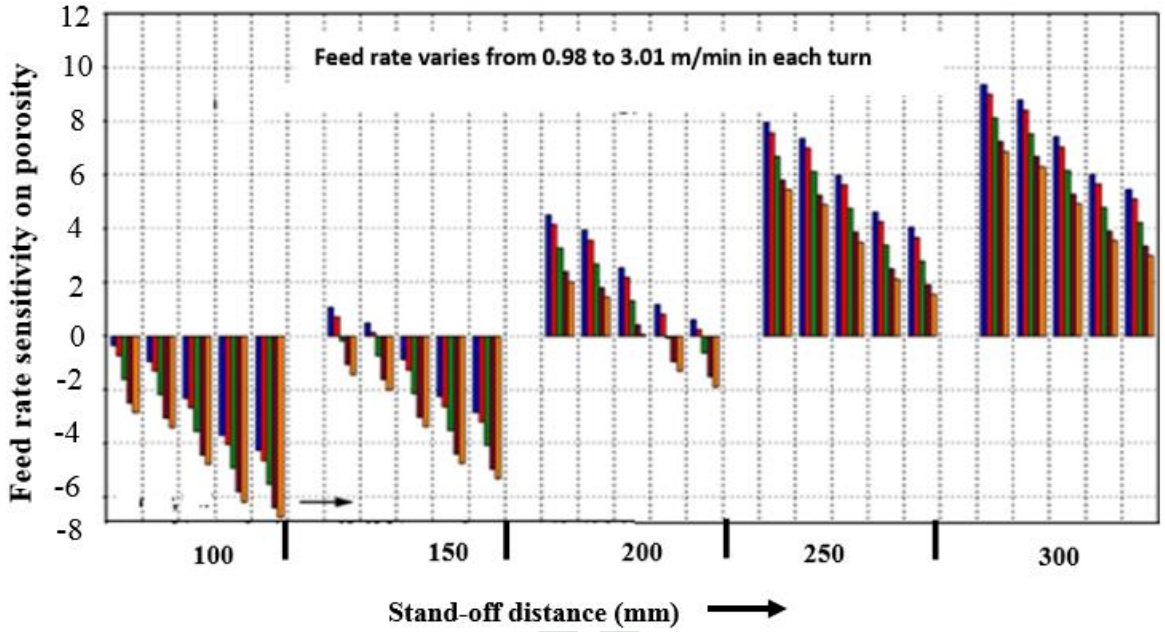

Figure 15 Wire feed rate sensitivity of porosity

V. CONCLUSIONS

The following important conclusions are obtained from this investigation:

- An empirical relationship is developed to predict the porosity level of electric arc sprayed Cp Ti coatings on Titanium alloy (Ti-6Al-4V), incorporating few important spray parameters. The developed relationship can be effectively used to predict the porosity level of Cp Ti coatings on Titanium alloy (Ti-6Al-4V) at 95% confidence level.
- A maximum porosity level of 36.75 vol. % could be attained under the electric arc spraying conditions of 7.6 kW of input power, 250 mm of stand-off distance and 1.86 m/min of wire feed rate and these parameters are found to be optimum spraying parameters with respect to maximizing porosity level in porous coatings.
- Input power was found to have greater influence on porosity of the coatings followed by stand-off distance and wire feed rate.
- Input power was found to be more sensitive than the other parameters such as stand-off distance and wire feed rate to the coating process.

REFERENCES

[1] B. Chang et al., "Influence of pore size of porous titanium fabricated by vacuum diffusion bonding of titanium meshes on cell penetration and bone ingrowth," Acta Biomater., vol. 33, pp. 311–321, Mar. 2016.

[2] G. Montavon, S. Sampath, C. C. Berndt, H. Herman, and C. Coddet, "Effects of the spray angle on splat morphology during thermal spraying," Surf. Coatings Technol., vol. 91, no. 1–2, pp. 107–115, May 1997.

[3] S. Van Bael et al., "The effect of pore geometry on the in vitro biological behavior of human periosteum-derived cells seeded on selective laser-melted Ti6Al4V bone scaffolds," Acta Biomater., vol. 8, no. 7, pp. 2824–2834, Jul. 2012.

[4] R.G. Miller; J.E. Freund ; D.E. Johnson, Probability and Statistics for Engineers, Prentice of Hall of India Pvt. Ltd., New Delhi. 1999.

[5] D.C. Montgomery; Design and Analysis of Experiments, John Wiley & Sons Ltd., New Delhi. 2007.

[6] "ASTM F1854-15:," Stereol. Eval. Porous Coatings Med. Implant. Am. Soc. Test. Mater., vol. 1, pp. 1–8, 2014.

[7] K. Y. Benyounis and A. G. Olabi, "Optimization of different welding processes using statistical and numerical approaches - A reference guide," Adv. Eng. Softw., vol. 39, no. 6, pp. 483–496, 2008.

[8] A. R. Hamad, J. H. Abboud, F. M. Shuaeib, and K. Y. Benyounis, "Surface hardening of commercially pure titanium by laser nitriding: Response surface analysis," Adv. Eng. Softw., vol. 41, no. 4, pp. 674–679, 2010.

[9] G. Box and N. Draper, Empirical model-building and response surfaces. 1987.

[10] Raymond H. Myers; Douglas C. Montgomery, Response Surface Methodology : Process and Product Optimization Using Designed Experiments. Wiley, 2016.

[11] J. Zhang and V. Desai, "Evaluation of thickness, porosity and pore shape of plasma sprayed TBC by electrochemical impedance spectroscopy," Surf. Coatings Technol., vol. 190, no. 1, pp. 98–109, Jan. 2005.

[12] A. Portinha et al., "Characterization of thermal barrier coatings with a gradient in porosity," Surf. Coatings Technol., vol. 195, no. 2–3, pp. 245–251, May 2005.

[13] V. Balasubramanian, A. K. Lakshminarayanan, R. Varahamoorthy, and S. Babu, "Understanding the Parameters Controlling Plasma Transferred Arc Hardfacing Using Response Surface Methodology," Mater. Manuf. Process., vol. 23, no. 7, pp. 674–682, 2008.

[14] J. Li, Y. Tian, Z. Huang, and X. Zhang, "Studies of the porosity in electroless nickel deposits on magnesium alloy," Appl. Surf. Sci., vol. 252, no. 8, pp. 2839–2846, Feb. 2006.

[15] A. S. Sarigül and A. Seçgin, "A study on the applications of the acoustic design sensitivity analysis of vibrating bodies," Appl. Acoust., vol. 65, no. 11, pp. 1037–1056, Nov. 2004.